View Online

Vibrational coherence in the excited state dynamics of $Cr(acac)_3$: probing the reaction coordinate for ultrafast intersystem crossing†

Joel N. Schrauben, Kevin L. Dillman, Warren F. Beck and James K. McCusker*

Received 12th April 2010, Accepted 29th May 2010
DOI: 10.1039/c0sc00262c

Vibrational coherence was observed following excitation into the lowest-energy spin-allowed $^4A_2 \rightarrow {}^4T_2$ ligand-field absorption of $Cr(acac)_3$. The transient kinetics were fit to a rapidly damped 164 cm^{-1} oscillatory component, the frequency of which is not associated with the ground state of the molecule. The signal is assigned as an excited-state vibrational coherence; the timescale of the event suggests that this vibrational coherence is retained during the $^4T_2 \rightarrow {}^2E$ intersystem crossing that immediately follows $^4A_2 \rightarrow {}^4T_2$ excitation. DFT calculations indicate that the 164 cm^{-1} oscillation likely corresponds to a combination of Cr–O bond stretching in the ligand-field excited state as well as large amplitude motion of the ligand backbone. This hypothesis is supported by ultrafast time-resolved absorption measurements on $Cr(t\text{-}Bu\text{-}acac)_3$ (where t-Bu-acac is the monoanionic form of 2,2,6,6-tetramethyl-3,5-heptanedione) – an electronically similar but more sterically encumbered molecule – which exhibits a $^4T_2 \rightarrow {}^2E$ conversion that is more than an order of magnitude slower than that observed for $Cr(acac)_3$. These results provide important insights into the nature of the reaction coordinate that underlies ultrafast excited-state evolution in this prototypical coordination complex.

Published on 25 June 2010 on http://pubs.rsc.org | doi:10.1039/C0SC00262C
Downloaded on 31 August 2010

Introduction

The development of ultrashort laser pulses has revolutionized the study of chemical dynamics by allowing detection of the formation and decay of transient species in chemical reactions that are triggered by the absorption of light.[1] One of the more widely examined phenomena deals with the creation of vibrational coherence, in which a system is excited with sufficient bandwidth to yield an in-phase superposition of multiple vibronic states (a so-called wavepacket). Even in large molecules, the vibrational modes associated with the reaction coordinate of photochemical transformations can be detected in terms of vibrational coherence either on the potential energy surface of the Franck–Condon state or on that of the product state.[1–21] In this report, we document an unusual observation of vibrational coherence in the excited ligand-field state manifold of a simple coordination complex. The data indicate that vibrational coherence is created upon impulsive excitation and is retained during the course of an ultrafast intersystem crossing (ISC) event. More significantly, an analysis of these observations coupled with results on a related compound have provided unique insights into the nature of the vibrational mode(s) coupled to the excited-state dynamics, in effect allowing us to identify the reaction coordinate associated with this sub-picosecond photophysical transformation.

Department of Chemistry, Michigan State University, East Lansing, MI, 48824, USA. E-mail: jkm@chemistry.msu.edu; Tel: +001-517-355-9715 ext. 106

† Electronic supplementary information (ESI) available: Kinetic traces for $Cr(acac)_3$ at different probe wavelengths, ground-state absorption spectrum of $Cr(t\text{-}Bu\text{-}acac)_3$ in CH_2Cl_2 solution and description of the data work-up and fitting procedures. See DOI: 10.1039/c0sc00262c

Experimental section

Sample preparation

General. $Cr(acac)_3$ was purchased from Aldrich and recrystallized twice from benzene/petroleum ether. All spectroscopic samples were prepared using spectrographic grade acetonitrile or dichloromethane.

Synthesis of tris(2,2,6,6-tetramethyl-3,5-heptanedionato)chromium(III), $Cr(t\text{-}Bu\text{-}acac)_3$. The synthesis of this compound was carried out *via* modification of a literature preparation.[22] To a solution of 2 ml water and 2 ml dioxane was added 0.6 g of urea (excess), 0.184 g (1 mmol, 0.208 ml) of 2,2,6,6-tetramethyl-3,5-heptanedione, and 0.089 g (0.33 mmol) of chromium(III) chloride hexahydrate. The reaction was refluxed for 3 days and the product washed with water and recrystallized from benzene/petroleum ether. Anal. Calcd for $C_{33}H_{57}CrO_6$: C 65.86, H 9.55; found C 65.85, H 9.29%.

Physical measurements

Time-resolved transient absorption data were collected using a one-color femtosecond pump–probe transient absorption instrument in the Beck laboratory that employs the dynamic-absorption approach of Shank and co-workers, where the probe beam is dispersed in a monochromator after passing through the sample.[3,4,23] The experiments were conducted with 50 fs pump and probe pulses (15 nm FWHM) centered at 600 nm. The detected probe bandpass selected by the monochromator was tuned either to the blue or red of the center of the pump spectrum; data were also acquired using the entire spectrum of the probe beam. Solutions of $Cr(acac)_3$ were prepared with an absorbance of approximately 0.7 at 600 nm in a 1 mm quartz

View Online

Published on 25 June 2010 on http://pubs.rsc.org | doi:10.1039/C0SC00262C
Downloaded on 31 August 2010

cuvette. The solution was flowed during the course of the experiment in order to mitigate the effects of thermal lensing. Additional details concerning the experimental procedures, data work-up and fitting to kinetic models are described in the ESI.†

Additional time-resolved absorption data were acquired on Cr(t-Bu-acac)$_3$ using a ~100 fs instrument that has been described previously;[24] additional details can be found in the ESI.† Due to limited solubility in CH_3CN, measurements on this compound were carried out in dichloromethane.[25] Sample absorbances were in the range of 0.5–0.7 in a 1 mm pathlength optical cuvette.

DFT calculations were carried out using Gaussian 98 at the UBLYP/6-311G** level, employing a CPCM solvent model for acetonitrile.[26] Vibrational modes were visualized using Gaussview.[27]

Results and discussion

The compound of interest in this report is tris(acetylacetonate)-chromium(III) (Cr(acac)$_3$). This system was chosen because of its well-documented photophysical properties,[28,29] high symmetry, and low quantum yield for photosubstitution (<0.01).[30] The relevant low-lying electronic structure of this compound can be understood in terms of (1) the ground state ($^4A_2$), arising from single occupancy of each of the three (nominally) t_{2g}-symmetry d-orbitals, (2) $(t_{2g})^2(e_g)^1$-based excited states ($^4T_2$ and a higher-energy $^4T_1$ term), and (3) a lower-energy ^2E state, corresponding to an intraconfigurational excited state of the $^4A_2$ term. The absorption and emission spectra of this compound are plotted in Fig. 1. Previous work from our group has documented solution-phase ultrafast dynamics associated with formation of the lowest-energy ^2E excited state of this compound.[24] Following $^4A_2 \rightarrow {}^4T_2$ excitation in the mid-visible, intersystem crossing (ISC) to the ^2E state occurs with a rate constant $k_{ISC} > 10^{13}$ s^{-1}; subsequent vibrational relaxation in the ^2E state was inferred from spectral narrowing to occur with a time constant of $\tau_{VR} \sim 1$ ps. Variable excitation-wavelength studies further suggested that bluer pump wavelengths resulted in population of higher-lying vibrational levels of ^2E, indicating that thermalization within the $^4T_2$ state is not kinetically competitive with ISC. This model was expanded upon through a recent ultrafast IR study by Kunttu and co-workers[31,32] who demonstrated that *ca.* 70–85% of the ground state is recovered *via* a thermally-induced back-intersystem crossing (BISC) to the quartet manifold (presumably the $^4T_2$ state), which then undergoes internal conversion on a 15 ps timescale to reform the ground state. The remaining ^2E population relaxes back to the ground state on a timescale of 760–900 ps, consistent with our previous report.[24] The results from both sets of experiments are summarized in the Jablonski diagram shown in Fig. 2. Given that only an upper limit for the time constant for ISC was defined through these experiments (<100 fs), we sought to obtain a more quantitative assessment of this process by enhancing the temporal resolution of the measurement.

Transient absorption data were acquired following irradiation into the $^4A_2 \rightarrow {}^4T_2$ absorption of Cr(acac)$_3$ at 600 nm. This wavelength corresponds to the low-energy shoulder of the band (Fig. 1): excitation therefore results in the preparation of a (relatively) cool Franck–Condon state on the $^4T_2$ potential energy surface. A positive transient feature was observed, consistent with our previous results showing a net excited-state absorption for the ^2E excited state of Cr(acac)$_3$ in the *ca.* 450–650 nm region.[24] A closer examination of the data revealed an oscillation superimposed on this excited-state absorption (Fig. 3). The feature can be described by two components, one having a frequency of 164 ± 20 cm^{-1} with a damping time constant of $\tau_{damp} = 70$ fs, and a second, much weaker component of 75 ± 25 cm^{-1} ($\tau_{damp} = 1.6$ ps). This observation is a clear indication of vibrational coherence associated with the photo-induced dynamics of Cr(acac)$_3$.

In recent years, vibrational coherence has been observed in a number of transition metal-based systems: examples include

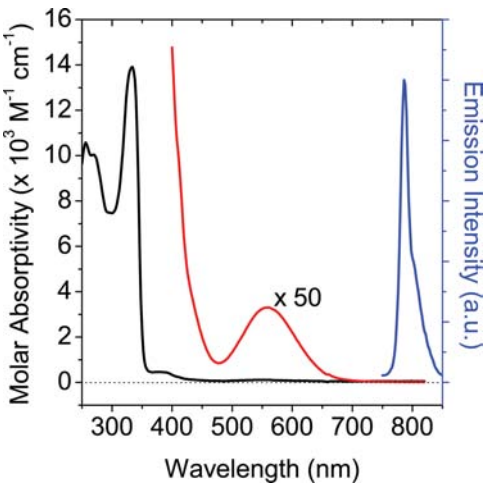

Fig. 1 Electronic absorption and emission spectra of Cr(acac)$_3$. The absorption spectrum was acquired in acetonitrile solution, whereas the emission spectrum was obtained at 80 K in a 4 : 1 EtOH/MeOH optical glass. The broad, low-intensity absorption feature centred at 560 nm corresponds to the $^4A_2 \rightarrow {}^4T_2$ absorption, while emission arises from the lowest-lying ^2E excited state.

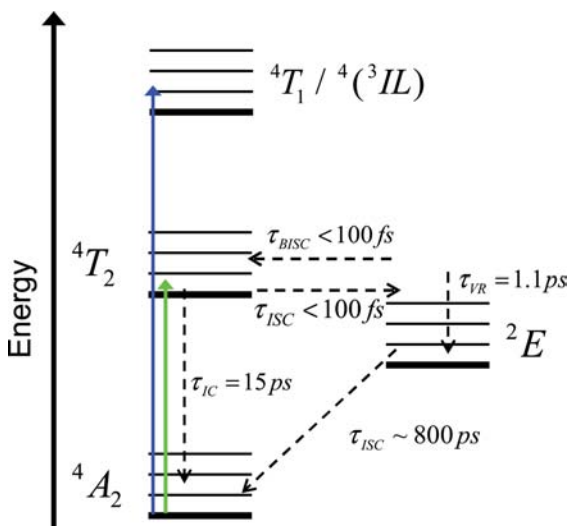

Fig. 2 Jablonski diagram summarizing the dynamics of Cr(acac)$_3$ in solution following excitation into the ligand field-state manifold.

This journal is © The Royal Society of Chemistry 2010

View Online

Published on 25 June 2010 on http://pubs.rsc.org | doi:10.1039/C0SC00262C
Downloaded on 31 August 2010

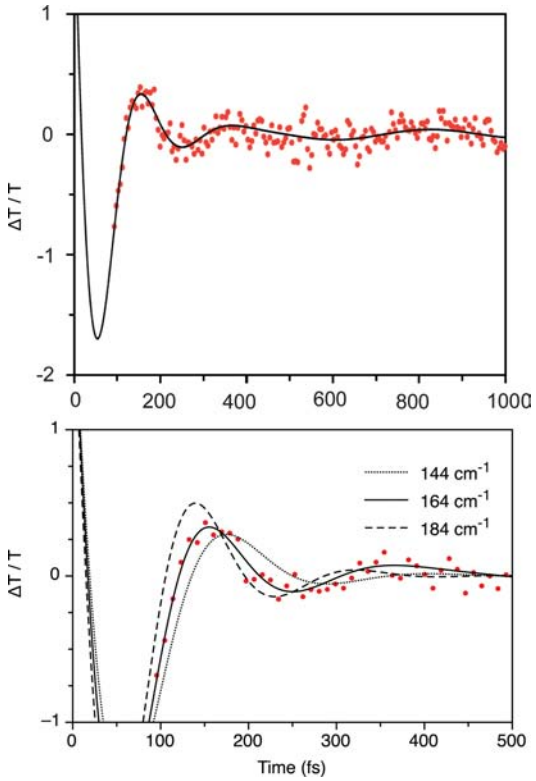

Fig. 3 *Top*: Single wavelength kinetic trace of $Cr(acac)_3$ at 592 ± 2 nm following excitation at 600 nm. An underlying increase in excited-state absorbance ($\tau = 320$ fs) was subtracted from the experimental data in the trace shown above in order to more clearly illustrate the oscillatory signal. The solid line corresponds to a fit of the data to two components: see text for further details. *Bottom*: Sample fits of the data shown in the top panel to oscillations with frequencies of 144 cm^{-1}, 164 cm^{-1}, and 184 cm^{-1}. The level of agreement suggests that the frequency can be considered reasonably well defined with $\omega_1 = 164 \pm 20$ cm^{-1}.

zinc porphyrins,[8,33] heme complexes,[5,34,35] other metalloproteins,[36] as well as mixed valence compounds.[7,20] Vibrational coherence has been less commonly observed in simple coordination complexes; one of the most compelling recent examples comes from optical studies of $[Fe(bpy)_3]^{2+}$ reported by Chergui and co-workers.[21] In most cases vibrational coherence is associated with a single electronic state, either the initially populated excited state (so called impulsive absorption) or the ground state (formed *via* impulsive stimulated Raman scattering).[2,7,33] Indirect vibrational coherence mechanisms have also been identified resulting from photochemistry,[5,11,13,14,37] rapid geometric changes,[21] or formation of some other type of product state.[22,32] Distinct from these processes is so-called retention of vibrational coherence, wherein a vibrational wavepacket is formed on one electronic surface and propagates through a barrier or avoided crossing to populate another electronic state with the wavepacket still intact. This phenomenon has been observed during internal conversion in cyanine dye molecules,[16] photochemical rearrangements,[17] photoisomerization,[18,19] and mixed valence species.[20]

The insufficient sensitivity of the instrument to detect modulation by wavepackets on the ground state, as a result of the low oscillator strength of the ground state ligand field absorption, eliminates the possibility that our observation results from vibrational coherence on the ground state surface. However, the excited state absorption, which is charge transfer in nature, provides sufficient oscillator strength to allow one to observe excited state vibrational coherence. This, coupled with the much longer timescales for ground-state recovery (*via* the $^4T_2$ and ^2E states as discussed above) strongly implies that the observed vibrational coherence is associated with the excited state(s) of the molecule. Our previous study of this system defined an upper limit for ISC of *ca.* 100 fs. Given that the oscillatory component in Fig. 3 is evident at time delays past 400 fs, we conclude that the wavepacket initially created in the $^4T_2$ state upon excitation persists upon formation of the ^2E state, *i.e.*, vibrational coherence is retained during ISC; in this regard it is tempting to view the damping time constant of ~70 fs as being reflective of this surface-crossing event.

Alternatively, vibrational coherence on the ^2E surface could result from an indirect mechanism such as the one implicated for $[Fe(bpy)_3]^{2+}$ in which vibrational coherence is associated with the lowest-energy excited state of the molecule (a $^5T_2$ ligand-field state).[21] Chergui and co-workers note that the oscillation of 130 cm^{-1} is likely due to N–Fe–N bending modes which are coherently excited by the impulsive Fe–N elongation that accompanies the transition from a low-spin to a high-spin state in that system. In the case of $Cr(acac)_3$ one would also expect significant geometric distortions along the Cr–O bonds in the $^4T_2$ excited state, however, there are two important distinctions to consider. First, in $Cr(acac)_3$ it is the initial (as opposed to the final) state that is characterized by an increased equilibrium metal–ligand bond distance: the ^2E product state is an intra-configurational term arising from a spin flip within the t_{2g} orbital set and thus presents an excited-state potential that is essentially nested with respect to the ground-state $^4A_2$ term. Second, the degree of distortion associated with the $^4T_2$ term should be significantly smaller than that of the $^5T_2$ term of $[Fe(bpy)_3]^{2+}$ due to the difference in valence configuration (*i.e.*, $(t_{2g})^4 (e_g)^2$ for high-spin Fe^{II} *versus* $(t_{2g})^2 (e_g)^1$ for the $^4T_2$ state of Cr^{III}). Given these considerations, the fact that the vibrational coherence appears to be present at or near $\Delta t = 0$, and the vibrationally cool nature of the initially prepared state makes retention of vibrational coherence a more compelling mechanistic assignment in the present case.

Retention of vibrational coherence during the $^4T_2 \rightarrow {}^2E$ conversion suggests that the vibrational mode(s) giving rise to the oscillations evident in Fig. 3 define the reaction coordinate for ultrafast ISC in this complex. In terms of identifying these modes, we start with the work of Perkovic and Endicott which implicated low-frequency modes as playing an important role in $^2E \rightarrow {}^4A_2$ conversion of Cr(III) complexes.[38] These workers concluded that systems that were sterically constrained along torsional degrees of freedom tended to exhibit slower rates of ISC relative to compounds with greater flexibility. In a non-constrained system, low-frequency modes result in a trigonal distortion of the compound; it can be shown that such a distortion results in extensive mixing of the d orbitals which would facilitate ISC.[39,40] Limiting motion along these coordinates would amount to the introduction of a barrier along this pathway, thereby slowing the kinetics of surface crossing. Although this model was developed based on data associated

View Online

Published on 25 June 2010 on http://pubs.rsc.org | doi:10.1039/C0SC00262C
Downloaded on 31 August 2010

with ground-state recovery, it is reasonable to consider a similar reaction coordinate coupling the $^4T_2$ and ^2E states in the ultrafast ISC of $Cr(acac)_3$.

In order to gain further insight into the nature of the low-energy vibrational structure of this system, we carried out ground-state DFT frequency calculations on $Cr(acac)_3$.[41–50] Of the several low-frequency modes that were identified from the calculations, two are of particular note: a symmetric breathing mode at 184 cm^{-1}, as well as a torsional "scissor" mode at 256 cm^{-1}. These calculated frequencies are in very good agreement with bands at 188 cm^{-1} and 254 cm^{-1} observed in the Raman spectrum of the compound (Fig. S4†). Drawings of these two modes are provided in Fig. 4. It can be seen that both of these ground-state vibrational modes involve displacements of the primary coordination sphere. The potential surface initially accessed upon excitation should be characterized by a smaller vibrational force constant than the ground state due to the interconfigurational nature of the $^4T_2$ term: both of these ground-state vibrational modes are therefore reasonable candidates for the origin of the 164 cm^{-1} vibrational coherence in Fig. 3.[50] Additional vibrational modes were identified at lower energies, nearly all of which, like those shown in Fig. 4, also involve large-amplitude motion of the peripheral methyl groups and/or twisting of the backbone of the acetylacetonate ligand. These observations suggest an experimental probe of the mechanism of ultrafast ISC, namely the use of sterics to modulate motion along this proposed reaction coordinate.

As a test of this hypothesis, we carried out ultrafast time-resolved absorption measurements on $Cr(t\text{-Bu-acac})_3$, where t-Bu-acac is 2,2,6,6-tetramethyl-3,5-heptanedione. This compound essentially replaces the peripheral methyl groups of acac with bulkier *tert*-butyl groups, thereby increasing the degree of steric interactions associated with the modes depicted in Fig. 4 without significantly affecting the zero-point energies of the electronic states involved in the ISC process. Time-resolved absorption data were acquired on $Cr(t\text{-Bu-acac})_3$ in fluid solution following excitation on the low energy shoulder of the $^4A_2 \rightarrow {}^4T_2$ absorption. The full differential absorption spectra are shown in Fig. 5A, along with data on $Cr(acac)_3$ that we have previously reported (Fig. 5B).[24] The spectral profile for $Cr(t\text{-Bu-acac})_3$ at the longest time delay shown (*i.e.*, $\Delta t = 12$ ps) is

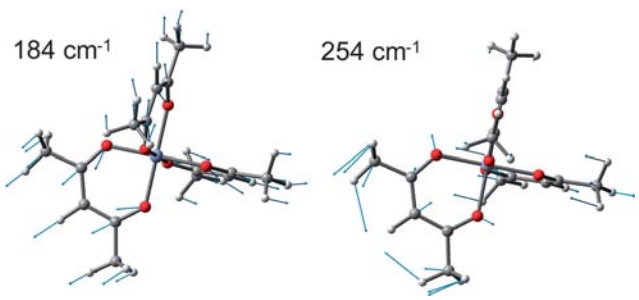

Fig. 4 Illustrations of the symmetric breathing and torsional "scissor" modes of $Cr(acac)_3$ based on a ground-state DFT frequency calculation. The calculation was carried out at the UBLYP/6-311G** level, employing a CPCM solvent model for acetonitrile. Both of these vibrational modes appear to involve large-amplitude displacements of the peripheral methyl groups of the ligand.

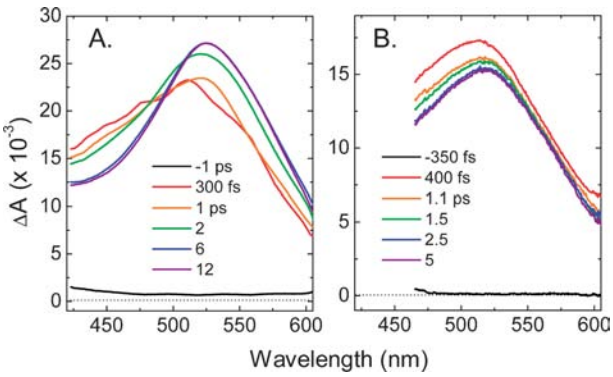

Fig. 5 (A) Differential absorption spectra of $Cr(t\text{-Bu-acac})_3$ in room-temperature CH_2Cl_2 solution following excitation at 633 nm; similar results were obtained following excitation at several additional wavelengths across the $^4A_2 \rightarrow {}^4T_2$ absorption envelope. (B) Differential absorption spectra acquired for $Cr(acac)_3$ in CH_3CN solution following excitation at 625 nm (reproduced from ref. 24).

invariant out to several hundred ps; this fact coupled with its similarity to the analogous data for $Cr(acac)_3$ confirm this transient as originating from the ^2E excited state of the compound. In contrast to the data on $Cr(acac)_3$, the data on $Cr(t\text{-Bu-acac})_3$ are characterized by significant changes in the overall profile of the differential absorption spectra at early times. Single-wavelength kinetic traces for $Cr(t\text{-Bu-acac})_3$ are plotted in Fig. 6. Consistent with the spectral evolution evident in Fig. 5A, data at 450 nm reveal a decay in the excited state absorption, whereas an increase in excited-state absorption is evident at 550 nm. The fitted time constants are slightly different at the two probe wavelengths, but are likely within experimental error (*i.e.*, $\tau \sim 1.8 \pm 0.4$ ps).

One can envision two distinct models for describing these data: (1) dynamics taking place on a single potential energy surface, which given the data at $\Delta t = 12$ ps means vibrational relaxation in the ^2E state, or (2) dynamics corresponding to a change in electronic structure, in this case conversion from the initially formed $^4T_2$ state to the ^2E. The first model is the one we

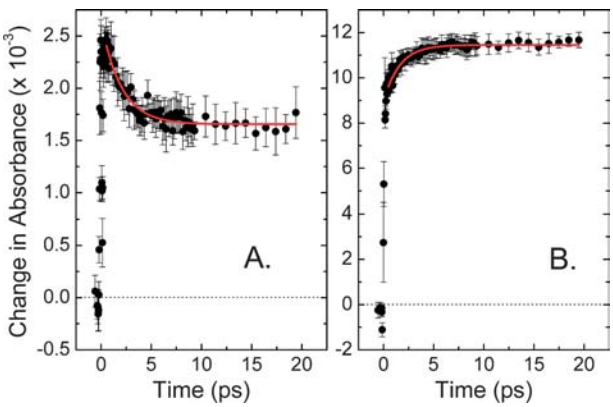

Fig. 6 Select single wavelength kinetic traces of $Cr(t\text{-Bu-acac})_3$ in CH_2Cl_2 solution at 450 nm (A) and 550 nm (B) following excitation at 610 nm. The solid lines correspond to fits of the data to single-exponential kinetic models ($\tau_{obs} = 2.0 \pm 0.2$ ps and 1.6 ± 0.2 ps for traces A and B, respectively).

This journal is © The Royal Society of Chemistry 2010

View Online

Published on 25 June 2010 on http://pubs.rsc.org | doi:10.1039/C0SC00262C
Downloaded on 31 August 2010

previously invoked to describe the time-dependent data for $Cr(acac)_3$;[24] the second would imply a significant reduction in the rate of ISC for $Cr(t\text{-}Bu\text{-}acac)_3$ relative to $Cr(acac)_3$. In distinguishing these two possibilities, we are guided by the general principle that, since vibrational relaxation does not involve a change in electronic structure, its overall effect on the profile of a differential absorption spectrum should be limited.[51] In contrast, a change from one electronic state to another will likely give rise to new absorption features associated with the product state at the expense of features characteristic of the initial state. In this context, we note that the qualitative difference in the spectral evolution of the two compounds being considered here is striking: whereas $Cr(acac)_3$ exhibits only a slight degree of spectral narrowing, the data for $Cr(t\text{-}Bu\text{-}acac)_3$ reveal a much broader, asymmetric spectral profile at early times which narrows, undergoes a significant red shift, and increases in intensity; by 12 ps, we observe an absorption band that is identical in all respects to that of $Cr(acac)_3$. This pronounced difference in the nature of the observed spectral changes between the two compounds compels us to ascribe the data on $Cr(t\text{-}Bu\text{-}acac)_3$ to a direct observation of the $^4T_2 \rightarrow {}^2E$ conversion in this compound.

To further substantiate this two-state kinetic model, we carried out a Gaussian deconvolution of the differential absorption data of $Cr(t\text{-}Bu\text{-}acac)_3$. Our analysis presumed the presence of a single absorption band arising from each electronic state. The spectra at long delay times (*i.e.*, $\Delta t > 10$ ps) can be described by a single Gaussian centered at 19 050 cm^{-1} (525 nm) with a full width at half-maximum (FWHM) of ~1200 cm^{-1}: this corresponds to the spectral signature of the ^2E state of $Cr(t\text{-}Bu\text{-}acac)_3$. Data at earlier delay times requires inclusion of a second band centered at 21 500 cm^{-1} (465 nm) with a FWHM = 1750 cm^{-1}. A plot of the deconvolution for the differential spectrum at $\Delta t = 2$ ps is shown in Fig. 7A as an example. Allowing only for changes in the relative areas of the two bands (*i.e.*, keeping constant the absorption maxima, band shape, and absorption cross-sections of the two Gaussians), one can easily reproduce the data on $Cr(t\text{-}Bu\text{-}acac)_3$ (Fig. 7B). At the earliest delay time ($\Delta t = 300$ fs) the integrated signal has roughly equal contributions from both the high-energy and low-energy features; subsequent spectra are characterized by a decay of the band at 465 nm concomitant with the growth of the absorption at 525 nm.

Despite the simplicity of this model, the spectral evolution observed for $Cr(t\text{-}Bu\text{-}acac)_3$ can clearly be described in terms of a conversion from one absorption profile to another. Specifically, we suggest that the feature near 465 nm in the deconvolved spectra corresponds to absorption(s) associated with the $^4T_2$ state; the decay of this feature thus reflects depopulation of the $^4T_2$ state as a result of conversion to the ^2E state of the compound. It should be emphasized that we have no knowledge concerning the relative oscillator strengths of the excited-state absorption features for this compound: we therefore cannot provide a quantitative assessment as to what the relative areas of the deconvolved contributions imply concerning population distributions. Nevertheless, within the context of this model, the observed time constant corresponds to the rate of intersystem crossing. Replacing the peripheral methyl groups in $Cr(acac)_3$ with *tert*-butyl groups in $Cr(t\text{-}Bu\text{-}acac)_3$ has therefore decreased the rate of ISC by more than an order of magnitude. While we

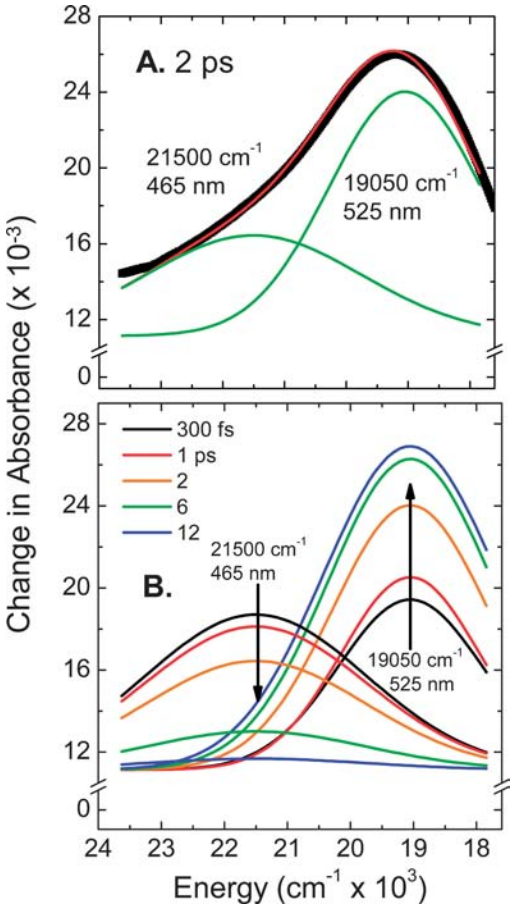

Fig. 7 Gaussian deconvolution of the transient full spectra of $Cr(t\text{-}Bu\text{-}acac)_3$ shown in Fig. 5A. An example fit for the transient spectrum at 2 ps is shown in panel A, whereas fits to the time-dependent spectral evolution are illustrated in panel B. See text for further details.

cannot at this stage be too specific in terms of which normal modes are dominant,[50] we believe these results lend considerable credibility to the notion that the sorts of low-frequency vibrational modes discussed above are indeed those driving ultrafast intersystem crossing in this system.[52]

Conclusions

The work presented in this report provides compelling evidence that the reaction coordinate of the ultrafast intersystem crossing process in $Cr(acac)_3$ has been identified. Following excitation into the $^4A_2 \rightarrow {}^4T_2$ ligand-field absorption of the compound, vibrational coherence was observed superimposed on the kinetics associated with excited-state evolution. DFT calculations suggested that the 164 cm^{-1} frequency of the observed oscillations was associated with Cr–O bond stretch vibrations that also involve large amplitude motions of the peripheral methyl groups of the ligand framework. This hypothesis was then tested through the ultrafast spectroscopic characterization of $Cr(t\text{-}Bu\text{-}acac)_3$, in which the peripheral methyl groups of the acac ligand were replaced by electronically similar but sterically bulkier *tert*-butyl groups. Time-resolved absorption data on $Cr(t\text{-}Bu\text{-}acac)_3$ revealed significant changes in the differential

View Online

absorption spectrum over the first several picoseconds following $^4A_2 \rightarrow {}^4T_2$ excitation, indicating that the rate of the $^4T_2 \rightarrow {}^2E$ intersystem crossing had been slowed by more than an order of magnitude relative to $Cr(acac)_3$ as a result of this compositional change to the system. We believe that these results constitute a significant step in our ongoing efforts to understand and ultimately control ultrafast excited-state dynamics of transition metal-based systems through the identification of the reaction coordinates associated with photo-induced transformations.

Acknowledgements

The authors would like to thank Prof. C. Reber and Alexandre Rodrigue-Witchel of Université de Montréal for the Raman spectrum of $Cr(acac)_3$. This work was supported with funds from the National Science Foundation through grant nos. CHE-0911592 (J.K.M.) and MCB-052002 (W.F.B.).

Published on 25 June 2010 on http://pubs.rsc.org | doi:10.1039/C0SC00262C
Downloaded on 31 August 2010

Notes and references

1 A. H. Zewail, *J. Phys. Chem. A*, 2000, **104**, 5660–5694.
2 K. R. Shelly, E. C. Golovich, K. L. Dillman and W. F. Beck, *J. Phys. Chem. B*, 2008, **112**, 1299–1307.
3 R. W. Schoenlein, L. A. Peteanu, R. A. Mathies and C. V. Shank, *Science*, 1991, **254**, 412–415.
4 S. L. Dexheimer, Q. Wang, L. A. Peteanu, W. T. Pollard, R. A. Mathies and C. V. Shank, *Chem. Phys. Lett.*, 1992, **188**, 61–66.
5 L. Zhu, J. T. Sage and P. M. Champion, *Science*, 1994, **266**, 629–632.
6 K. L. Dillman, K. R. Shelly and W. F. Beck, *J. Phys. Chem. B*, 2009, **113**, 6127–6139.
7 P. J. Reid, C. Silva, P. F. Barbara, L. Karki and J. T. Hupp, *J. Phys. Chem.*, 1995, **99**, 2609–2616.
8 M. Yoon, D. Jeong, S. Cho, D. Kim, H. Rhee and T. Joo, *J. Chem. Phys.*, 2003, **118**, 164–171.
9 W. T. Pollard, S. L. Dexheimer, Q. Wang, L. A. Peteanu, C. V. Shank and R. A. Mathies, *J. Phys. Chem.*, 1992, **96**, 6147–6158.
10 C. J. Bardeen, Q. Wang and C. V. Shank, *J. Phys. Chem. A*, 1998, **102**, 2759–2766.
11 P. M. Champion, F. Rosca, D. Ionascu, W. Cao and X. Ye, *Faraday Discuss.*, 2004, **127**, 123–135.
12 S. A. Trushin, W. Fuss, W. E. Schmid and K. L. Kompa, *J. Phys. Chem. A*, 1998, **102**, 4129–4137.
13 U. Banin, A. Waldmann and S. Ruhmann, *J. Chem. Phys.*, 1992, **96**, 2416–2419.
14 N. Pugliano, D. K. Palit, A. Z. Szarka and R. M. Hochstrasser, *J. Chem. Phys.*, 1993, **99**, 7273–7276.
15 I. V. Rubstov and K. Yoshihara, *J. Chin. Chem. Soc.*, 2000, **47**, 673–677.
16 T. Fuji, H. Jin Ong and T. Kobayashi, *Chem. Phys. Lett.*, 2003, **380**, 135–140.
17 S. Takeuchi and T. Tahara, *J. Phys. Chem. A*, 2005, **109**, 10119–10207.
18 T. Kobayashi, T. Saito and H. Ohtani, *Nature*, 2001, **414**, 531–534.
19 E. Lenderink, K. Duppen and D. A. Wiersma, *J. Phys. Chem.*, 1995, **99**, 8972–8977.
20 T. W. Marin, B. J. Homoelle, K. G. Spears and J. T. Hupp, *J. Phys. Chem. A*, 2002, **106**, 1131–1143.
21 C. Consani, M. Premont-Schwarz, A. ElNahhas, C. Bressler, F. van Mourik, A. Cannizzo and A. Chergui, *Angew. Chem., Int. Ed.*, 2009, **48**, 7184–7187.
22 Y. Jiang, M. Liu, Y. Wang, H. Song, J. Gao and G. Meng, *J. Phys. Chem. A*, 2006, **110**, 13479–13486.
23 H. L. Fragnito, J. Y. Bigot, P. C. Becker and C. V. Shank, *Chem. Phys. Lett.*, 1989, **160**, 101–104.
24 E. Juban and J. McCusker, *J. Am. Chem. Soc.*, 2005, **127**, 6857–6865.
25 Time-resolved absorption data for $Cr(acac)_3$ acquired in CH_2Cl_2 were identical to those obtained in CH_3CN, suggesting that solvent does not significantly influence the excited-state dynamics of this system.
26 M. J. Frisch, G. W. Trucks, H. B. Schlegel, G. E. Scuseria, M. A. Robb, J. R. Cheeseman, V. G. Zakrzewski, J. A. Montgomery, R. E. Stratmann, J. C. Burant, S. Dapprich, J. M. Millam, A. D. Daniels, K. N. Kudin, M. C. Strain, O. Farkas, J. Tomasi, V. Barone, M. Cossi, R. Cammi, B. Mennucci, C. Pomelli, C. Adamo, S. Clifford, J. Ochterski, G. A. Petersson, P. Y. Ayala, Q. Cui, K. Morokuma, D. K. Malick, A. D. Rabuck, K. Raghavachari, J. B. Foresman, J. Cioslowski, J. V. Ortiz, B. B. Stefanov, G. Liu, A. Liashenko, P. Piskorz, I. Komaromi, R. Gomperts, R. L. Martin, D. J. Fox, T. Keith, M. A. Al-Laham, C. Y. Peng, A. Nanayakkara, C. Gonzalez, M. Challacombe, P. M. W. Gill, B. Johnson, W. Chen, M. W. Wong, J. L. Andres, M. Head-Gordon, E. S. Replogle and J. A. Pople, *Gaussian 98*, Gaussian, Inc., Pittsburgh, PA, 1998.
27 *GaussView 2.1*, Gaussian, Inc., Pittsburgh, PA, 2000.
28 A. D. Kirk, *Chem. Rev.*, 1999, **99**, 1607–1640.
29 L. S. Forster, *Chem. Rev.*, 1990, **90**, 331–353.
30 E. Zinato, P. Riccieri and P. S. Sheridan, *Inorg. Chem.*, 1979, **18**, 720–724.
31 E. M. S. Macoas, R. Kananavicius, P. Myllyperkio, M. Pettersson and H. Kunttu, *J. Am. Chem. Soc.*, 2007, **129**, 8934–8935.
32 It should be noted that the data acquired by Kunttu and co-workers were obtained following excitation at 400 nm. This wavelength predominately excites the higher energy $^4A_2 \rightarrow {}^4T_1$ ligand-field band as opposed to the $^4A_2 \rightarrow {}^4T_2$ transition upon which the conclusions in ref. 24 were based.
33 K. L. Dillman, K. R. Shelley and W. F. Beck, *J. Phys. Chem. B*, 2009, **113**, 6127–6139.
34 F. Gruia, D. Ionascu, M. Kubo, X. Ye, J. Dawson, R. L. Osborne, S. G. Sligar, I. Denisov, A. Das, T. L. Poulos, J. Terner and P. M. Champion, *Biochemistry*, 2008, **47**, 5156–5167.
35 F. Rosca, A. T. N. Kumar, I. D., X. Ye, A. A. Demidov, T. Sjodin, D. Wharton, D. Barrick, S. G. Sligar, T. Yonetani and P. M. Champion, *J. Phys. Chem. A*, 2002, **106**, 3540–3552.
36 I. Delfino, C. Manzoni, K. Sato, C. Dennison, G. Cerullo and S. Cannistraro, *J. Phys. Chem. B*, 2006, **110**, 17252–17259.
37 S. A. Trushin, W. Fuss, W. E. Schmid and K. L. Kompa, *J. Phys. Chem. A*, 1998, **102**, 4129–4137.
38 M. W. Perkovic and J. F. Endicott, *J. Phys. Chem.*, 1990, **94**, 1217–1219.
39 A. Ceulemans, N. Bongaerts and L. G. Vanquickenborne, *Inorg. Chem.*, 1987, **26**, 1566–1573.
40 K. F. Purcell, *J. Am. Chem. Soc.*, 1979, **101**, 5147–5152.
41 K. Nakamoto, P. J. McCarthy and A. E. Martell, *J. Am. Chem. Soc.*, 1961, **83**, 1272–1276.
42 K. Nakamoto, C. Udovich and J. Takemoto, *J. Am. Chem. Soc.*, 1970, **92**, 3973–3976.
43 J. P. Dismukes, L. H. Jones and J. C. Bailar, *J. Phys. Chem.*, 1961, **65**, 792–795.
44 I. Diaz-Acosta, J. Baker, W. Cordes, J. F. Hinton and P. Pulay, *Spectrochim. Acta, Part A*, 2003, **59**, 363–377.
45 I. Diaz-Acosta, J. Baker, W. Cordes and P. Pulay, *J. Phys. Chem. A*, 2001, **105**, 238–244.
46 S. F. Tayyari and F. Milani-nejad, *Spectrochim. Acta, Part A*, 2000, **56**, 2679–2691.
47 S. F. Tayyari, H. Raissi and Z. Ahmaabadi, *Spectrochim. Acta, Part A*, 2002, **58**, 2669–2682.
48 H. Sato, T. Taniguchi, A. Nakahashi, K. Monde and A. Yamagishi, *Inorg. Chem.*, 2007, **46**, 6755–6766.
49 D. A. Thornton, *Coord. Chem. Rev.*, 1990, **104**, 173–249.
50 Frequency calculations for the $^4T_2$ and ^2E excited states of $Cr(acac)_3$ are currently in progress.
51 J. K. McCusker, *Acc. Chem. Res.*, 2003, **36**, 876–887.
52 Low-frequency metal–ligand modes have been implicated in the intersystem crossing dynamics of a Re-based complex. See: A. Cannizzo, A. M. Blanco-Rodriguez, A. E. Nahhas, J. Sebera, S. Zalis, A. Vlcek, Jr. and M. Chergui, *J. Am. Chem. Soc.*, 2008, **130**, 8967–8974.

 This journal is © The Royal Society of Chemistry 2010